Analytica Chimica Acta 1165 (2021) 338543

Contents lists available at ScienceDirect

Analytica Chimica Acta

journal homepage: www.elsevier.com/locate/aca

Ultrasensitive electrochemical detection of miRNA coupling tetrahedral DNA modified gold nanoparticles tags and catalyzed hairpin assembly

Hua Chai [a], Mingyuan Wang [c], Longhai Tang [c], Peng Miao [a, b, *]

[a] Suzhou Institute of Biomedical Engineering and Technology, Chinese Academy of Sciences, Suzhou, 215163, People's Republic of China
[b] Ji Hua Laboratory, Foshan, 528200, People's Republic of China
[c] Suzhou Blood Center, Suzhou, 215006, People's Republic of China

HIGHLIGHTS

- An ultrasensitive electrochemical biosensor for the detection of miRNA is developed.
- Tetrahedral DNA modified AuNPs tags are applied for signal enhancement.
- The electrochemical method successfully distinguishes target miRNA from mismatched miRNAs.
- The electrochemical method performs satisfactorily in clinical samples.

GRAPHICAL ABSTRACT

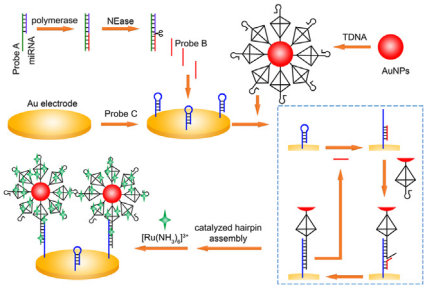

ARTICLE INFO

Article history:
Received 18 March 2021
Received in revised form
2 April 2021
Accepted 17 April 2021
Available online 22 April 2021

Keywords:
miRNA
Strand displacement
Catalyzed hairpin assembly
DNA tetrahedron
Chronocoulometry

ABSTRACT

MicroRNAs (miRNAs) play key regulatory roles in a number of biological processes, which act as critical biomarkers for clinical diagnosis. There are urgent needs to develop advanced tools for accurate and convenient analysis of miRNA in biological circumstances. In this study, an ultrasensitive electrochemical biosensor for miRNA assay is fabricated. Tetrahedral DNA modified gold nanoparticles tags are applied with optimized orientation, which are able to recruit a large number of electrochemical species for remarkable signal responses. Benefiting from the excellent amplification efficiency of the association of strand displacement amplification and catalyzed hairpin assembly, the established method shows ultrahigh sensitivity with the limit of detection as low as 10 aM. A wide linear range from 10^{-17} to 10^{-7} M is achieved. In addition, this method is capable to specifically discriminate interfering miRNAs with slightly different sequences. The successful assessment of miRNA levels in human serum samples also demonstrates good practical utility. Therefore, the proposed method has great potential to the applications of miRNA expression profiling and biological studies.

1. Introduction

MicroRNAs (miRNAs) are a type of small (approximately 18–25 nucleotides), noncoding endogenous RNAs [1,2]. They are post-transcriptional regulators of gene expression through repressing translation or mediating mRNA cleavage [3]. Accumulating

* Corresponding author. Suzhou Institute of Biomedical Engineering and Technology, Chinese Academy of Sciences, Suzhou, 215163, People's Republic of China.
E-mail address: miaopeng@sibet.ac.cn (P. Miao).

https://doi.org/10.1016/j.aca.2021.338543
0003-2670/

evidences have indicated miRNAs play significant roles in many important biological processes and their expression levels are closely associated with the occurrence and development of certain diseases [4–6]. For instance, miR-21 functions in cardiovascular diseases and many solid tumors [7,8]; miR-196b is overexpressed in the case of pancreatic cancer [9]; miR-15b is able to promote the progression of hepatocellular carcinomas [10]. Therefore, miRNA expression profiles can not only be used as critical biomarkers for disease diagnosis or screening, but also serve as powerful targets in drug discovery [11]. Despite the high analysis value on clinical researches, convenient and sensitive detection of miRNA is still challenging unlike other RNAs (e.g., mRNA, tRNA, lncRNA). The reason is that miRNAs possess certain intrinsic characteristics including small size, low abundance, and high sequence homology between family members [12,13].

Traditional analytical methods for RNA detection include northern blotting, microarray and reverse transcription polymerase chain reaction (RT-PCR) [14]. To date, a variety of techniques have been applied such as mass spectrometry [15], surface enhanced Raman scattering (SERS) [16], surface plasmon resonance (SPR) [17], fluorescence [18], and electrochemistry [19]. To meet the requirements raised by point-of-care diagnosis, more efforts should be made in the aspects of eliminating the use of expensive equipment, improving sensitivity, and so on. Isothermal amplification techniques are used to amplify the signal of a recognition event at constant temperature [20]. The experimental conditions are facile and the requirements for precise and complex instrument can be eliminated. A varieties of isothermal strategies have been developed, such as rolling circle amplification (RCA) [21], hybridization chain reaction (HCR) [22], strand displacement amplification (SDA) [23], catalytic hairpin assembly (CHA) [24], loop-mediated isothermal amplification (LAMP) [25], and so on.

In the present study, we demonstrate an ultrasensitive electrochemical method for the quantification of target miRNA based on isothermal amplification by SDA and CHA. In addition, tetrahedral DNA (TDNA), a typical three-dimensional DNA nanostructure, is introduced and conjugated with gold nanoparticles (AuNPs) as ideal scaffolds for reactions and amplified electrochemical tags. AuNPs possess the merits of easy synthesis, high loading capacity and excellent electric conductivity. The nanostructure of TDNA shows mechanical rigidity and structural stability. By modifying certain chemical substances, the orientation of TDNA on AuNPs is optimized to achieve the best electrochemical response. Under optimal conditions, the limit of detection for the analysis of miRNA is as low as 10 aM. In addition, the strategy has been successfully applied to analyze real biological samples with satisfactory results.

2. Experimental

2.1. Materials and instruments

Tris (2-carboxyethyl) phosphine (TCEP), mercaptohexanol (MCH), diethypyrocarbonate (DEPC), hexaammineruthenium(III) chloride ($[Ru(NH_3)_6]^{3+}$), and ethylenediaminetetraacetic acid (EDTA) were ordered from Sigma (USA). Chloroauric acid ($HAuCl_4$) was obtained from Shanghai Jiushan Chemicals Co., Ltd. (Shanghai, China). Klenow fragment polymerase, Nb.BbvCI nicking endonuclease (NEase), and deoxynucleotides (dNTPs) were purchased from New England Biolabs (Beijing, China). All other chemicals were of analytical grade without further purification. All oligonucleotides were ordered from Takara Biotechnology Co., Ltd. (Dalian, China). Their sequences and modifications were listed in Table S1. Human serum samples were collected from local hospital (Suzhou, China). qRT-PCR kit was ordered from Tiangen Biotech Co., Ltd. (Beijing, China). Water used in this work was purified by a Millipore water purification system (18 MΩ cm), which was treated with DEPC before use. Electrochemical measurements were performed on a CHI 660D electrochemical workstation (CH Instruments, China). Polyacrylamide gel image was taken by GelDoc XR$^+$ System (Bio-Rad, USA). qRT-PCR experiments were carried out on an ABI 7500 Real-Time PCR System (ABI Life Technologies, USA). UV–vis absorption spectra were recorded by a NanoDrop OneC spectrophotometer (Thermo Scientific, USA).

2.2. Preparation of DNA tetrahedron modified AuNPs

AuNPs with smaller diameter possess larger specific area for DNA modification. Considering the size of TDNA, AuNPs with the diameter of 13 nm were synthesized by citrate reduction of $HAuCl_4$ according to a previous report [26]. Generally, 3.5 mL of trisodium citrate with the concentration of 1% (w/v) was spiked into 100 mL of boiling $HAuCl_4$ solution. The reaction was lasted for 15 min under continued stirring. After that, the heat was removed and the solution was stirred for another 30 min. Then, the formed AuNPs were purified by two cycles of centrifuging at 12000 rpm for 30 min. Tetrahedral DNA (TDNA) was formed by the hybridization between four single-stranded DNA probes (Probe Ta, Tb, Tc and Td). The four probes with the concentrations of 12 μM were mixed in the buffer solution (10 mM Tris-HCl, 10 mM TCEP, 50 mM $MgCl_2$, pH 7.5). After heating to 95 °C for 5 min, the solution was cooled down slowly. 50 μL of TDNA was blended with 50 μL of AuNPs (30 nM). The mixture was transferred in the laboratory freezer at −20 °C. After reaction for 2 h, TDNA capped AuNPs were thawed at room temperature. Subsequently, the nanoconjugates were centrifuged at 12000 rpm for 30 min for purification.

2.3. Preparation of DNA modified electrode

The substrate working electrode (diameter: 2 mm) was firstly incubated with piranha solution (*Caution: highly corrosive*) for about 5 min. After rinsing carefully with pure water, the electrode was polished using silicon carbide paper (P5000) and then alumina powders (diameters: 1.0, 0.3, 0.05 μm), successively. Subsequently, it was ultasonicated in ethanol and double-distilled water, each for 5 min. The electrode was then treated with nitric acid (50%) for 30 min before electrochemically cleaned in 0.5 M H_2SO_4. After that, the electrode was rinsed again with pure water and incubated with 0.8 μM Probe C (10 mM Tris-HCl, 1 mM EDTA, 10 mM TCEP, 0.1 M NaCl, pH 7.4) for 9 h, followed by further treatment with 1 mM MCH (0.5 h) so as to achieve a well-aligned DNA monolayer.

2.4. Strand displacement amplification and catalyzed hairpin assembly

Standard target miRNA with a series of concentrations were firstly prepared. Probe A with the concentration of 2 μM was prepared in 20 mM Tris-acetate, 10 mM magnesium acetate, 50 mM potassium acetate, 100 μg mL^{-1} BSA (pH 7.9). Target miRNA was mixed with Probe A. In addition, 100 μM dNTPs, 0.3 unit μL^{-1} Nb.BbvCI and 0.06 unit μL^{-1} Klenow fragment polymerase were added. SDA reaction was carried out at 30 °C for 60 min, which was then terminated by heating to 85 °C for 20 min. Probe C modified electrode was immersed in the above solution for 30 min. After carefully rinsing with pure water, the electrode was further treated with TDNA modified AuNPs for 120 min.

2.5. Electrochemical measurements

A three-electrode system was used in this work, which consisted of a saturated calomel reference electrode, a platinum wire counter

electrode and the gold working electrode. Cyclic voltammetry (CV) and electrochemical impedance spectroscopy (EIS) were carried out using the electrolyte of 5 mM $[Fe(CN)_6]^{3-/4-}$ solution containing 1 M KNO_3. The parameters were as follows. For CV, the scan range was from +0.7 V to 0 V and the scan rate was 50 mV s^{-1}; for EIS, the biasing potential was 0.205 V, the amplitude was 5 mV and the frequency range was from 0.1 Hz to 100 kHz. Chronocoulometry (CC) was performed in the electrolyte of 10 mM Tris–HCl solutions (pH 7.4) containing 50 μM $[Ru(NH_3)_6]^{3+}$. The pulse period was 250 ms.

3. Results and discussion

3.1. Biosensing principle

Detailed working mechanism of this biosensor with multiple signal amplifications is illustrated in Scheme 1. Generally, SDA is firstly employed to amplify miRNA information. Probe A as the template hybridizes with target miRNA partially. After the cycles of extension, nicking digestion and displacement reactions, a number of Probe B are produced as the trigger of CHA, the second signal amplification procedure. Probe C, as one hairpin of CHA, is modified on the electrode surface via gold-sulfur chemistry. Another hairpin is designed on a stable TDNA nanostructure (hybridized by Probe Ta, Tb, Tc and Td) [27]. The successful synthesis of TDNA is confirmed by polyacrylamide gel electrophoresis. After the hybridization of the complementary sequences, three-dimensional DNA nanostructures with larger molecule weights are formed (Fig. S1). TDNA is then attached on the surface of AuNPs. The linkage relies on the thiol group modified on the vertex of TDNA (Probe Ta). Since $[Ru(NH_3)_6]^{3+}$ can be electrostatically bound to the phosphate backbone of DNA, the three-dimensional scaffold shows much greater capability to enrich $[Ru(NH_3)_6]^{3+}$, which benefits the enhancement of electrochemical response. In the presence of produced Probe B, CHA reaction occurs by subsequently opening the hairpin structures of Probe C and Probe Tb. Probe B is displaced and recycled in more CHA reactions. Finally, a large number of TDNA modified AuNPs can be localized on the surface of electrode to capture $[Ru(NH_3)_6]^{3+}$, which provide significant electrochemical signal (CC) to probe target miRNA [28].

3.2. Electrochemical characterization

Electrochemical properties of the modified electrode during different reaction stages are investigated by CV, EIS and CC, respectively. As shown in Fig. 1A, pairs of well-defined current peaks are displayed. After the incubation of TDNA modified AuNP directly, the intensities of the peaks decrease slightly, which are due to non-specific adsorption. Similarly, the direct incubations with Probe A or SDA product cannot lead to significant decrease of current peaks. However, after miRNA initiated SDA and CHA, TDNA modified AuNPs can be immobilized. The enrichment of DNA on the electrode results in remarkable decrease of current peaks. EIS results are consistent with CV results. As shown in Fig. 1B, with the complete procedures of SDA and CHA, a large number of DNA molecules are immobilized, which repels $[Fe(CN)_6]^{3-/4-}$ significantly, leading to a larger semicircle domain of nyquist plot [29]. $[Ru(NH_3)_6]^{3+}$ is another electrochemical species for qualitative and quantitative analysis. The measurement of $[Ru(NH_3)_6]^{3+}$ response relies on CC. The redox charge (Q) can be calculated from the chronocoulometric intercept at $t = 0$. Thus higher curves of CC indicate larger Q values. After comparison, Q values after independent incubations of AuNPs, Probe A or SDA product are relatively low, demonstrating insufficient immobilization of DNA molecules to adsorb $[Ru(NH_3)_6]^{3+}$ (Fig. 1C).

We have then studied the effect of orientation of TDNA on AuNPs. Probe Tc* and Td* labeled with thiols are employed, thus the constructed TDNA possesses three thiolated vertexes. Via gold-sulfur chemistry, this specific TDNA (termed bTDNA) interacts with AuNPs based on the bottomed three vertexes. Instead, the

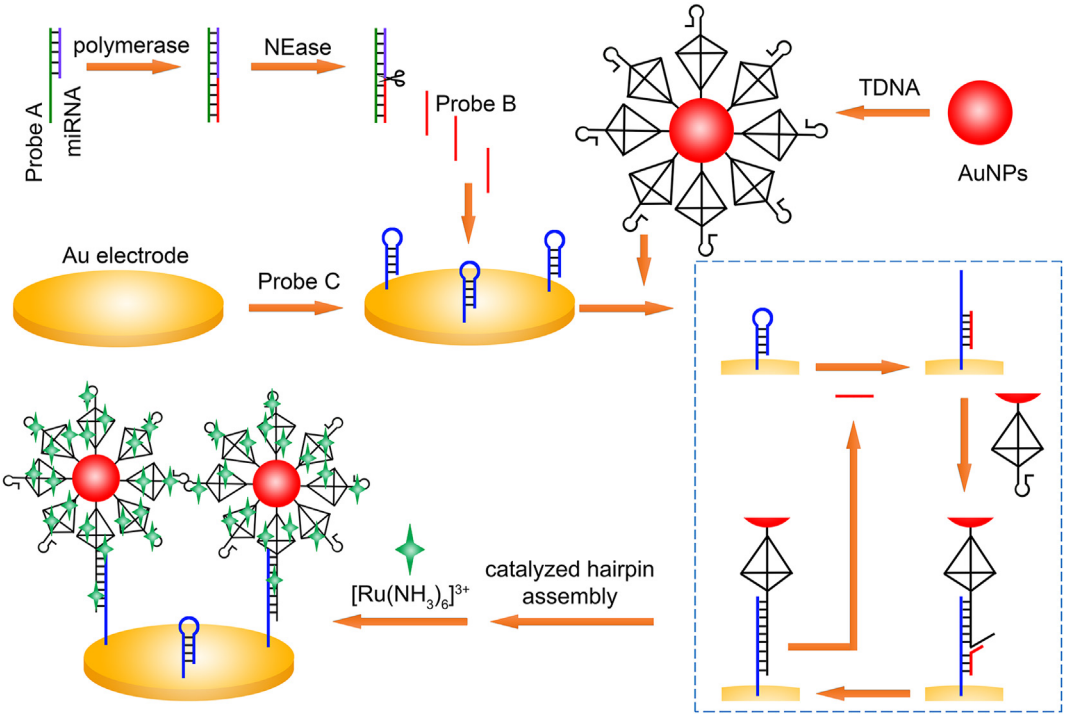

Scheme 1. Illustration of the electrochemical biosensor for miRNA assay based on TDNA modified AuNPs tags and catalyzed hairpin assembly.

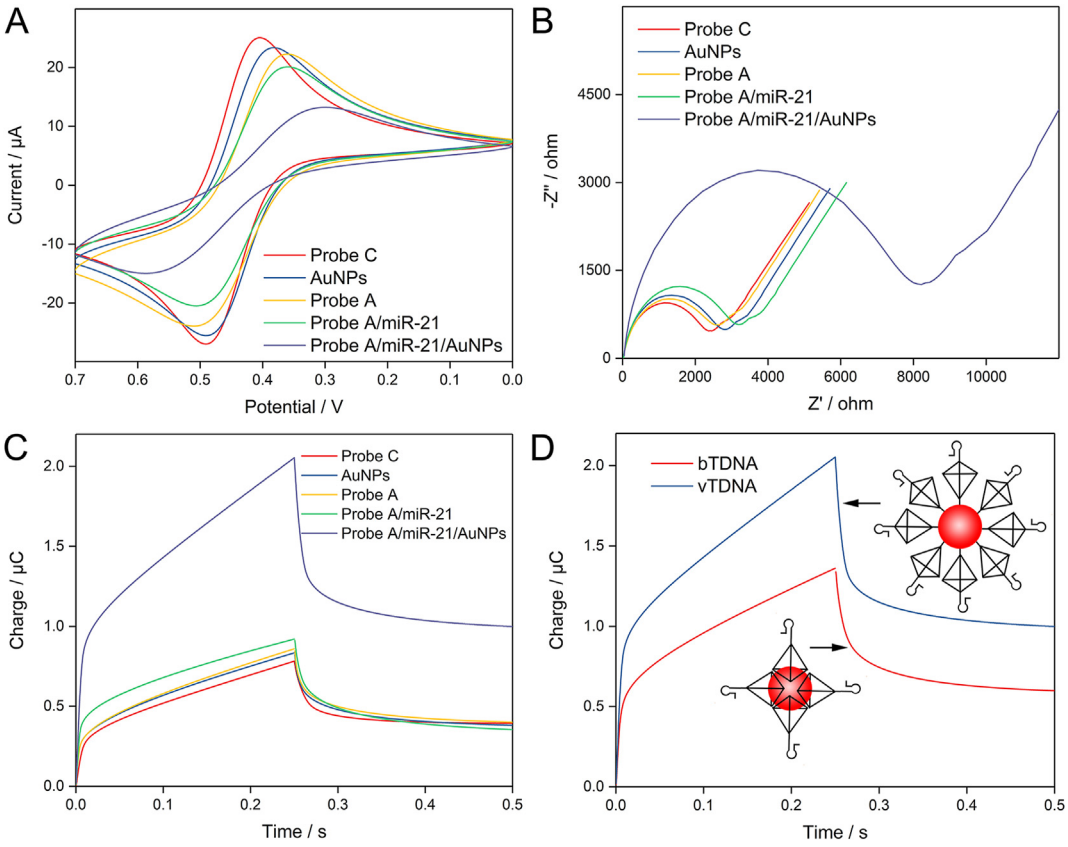

Fig. 1. (A) Cyclic voltammograms, (B) nyquist diagrams and (C) chronocoulometry diagrams of Probe C modified electrode, after incubation with TDNA modified AuNPs, after incubation with Probe A for SDA in the absence and presence of miRNA, after further incubation with AuNPs. (D) Chronocoulometry curves for the detection of miRNA using AuNPs modified with bTDNA and vTDNA, respectively.

orientation of TDNA (Probe Ta, Tb, Tc and Td) is different, in which only one thiolated vertex is utilized to link TDNA and AuNPs. Thus it is termed vTDNA. DNA density around AuNPs is supposed to be much larger for vTDNA than bTDNA. As expected, in the UV–vis absorption spectra, vTDNA modified AuNPs shows a larger peak around 260 nm (Fig. S2). Therefore, after immobilized on electrode, vTDNA modified AuNPs are able to recruit more $[Ru(NH_3)_6]^{3+}$ for signal output. As shown in Fig. 1D, the CC curve for vTDNA modified AuNPs indeed appears higher than that of bTDNA modified AuNPs. Q values are calculated to be 0.68 and 0.42C respectively, indicating that orientation of vTDNA benefits higher electrochemical response.

3.3. Experimental optimizations and electrochemical quantification of miRNA

To reach optimal analytical performance of this electrochemical biosensor, the concentration of Probe C for electrode modification, the times of SDA and CHA reactions are separately optimized. R_{ct} value can reflect the modification degree of DNA layer on the electrode interface. Therefore, we have monitored EIS results of the electrode modified with different concentrations of DNA (Fig. S3). With the increase of Probe C from 0.2 to 0.8 μM, more DNA molecules are immobilized and the R_{ct} becomes steady around 2600 Ω. Therefore, 0.8 μM is used for the following experiments. Usually, longer reaction time is able to produce larger signal output. We have then checked the redox charge of $[Ru(NH_3)_6]^{3+}$ (Q) in CC curves with different reaction times of SDA and CHA. As longer times of reactions, Q values increase and reach corresponding plateaus (Fig. S4). Accordingly, we have chosen 60 min (SDA) and 120 min (CHA) for the following experiments, respectively.

Under these optimum conditions, electrochemical responses of vTDNA modified AuNPs tags immobilized on electrode triggered by different concentrations of miRNA are recorded to evaluate the sensing performances. As expected, CC curve becomes higher with the incremental concentration of miR-21 (Fig. 2A), and the redox charge of $[Ru(NH_3)_6]^{3+}$ (Q) shows a positive correlation with the logarithmic concentration of miRNA (Fig. 2B). The linear range is from 10^{-17} to 10^{-7} M, which is quite wide. The equation is as follows:

$$y = 0.922 + 0.043\,x\ (n = 3,\ R^2 = 0.997)$$

in which, y strands for the Q value and x is the logarithmic concentration of miRNA. The limit of detection is evaluated to be 10 aM at a signal-to-noise ratio (S/N) of 3, which is better or at least comparable with recently developed methods for the detection of miRNA (Table 1).

3.4. Selectivity investigation and serum assay

The characteristic of high sequence homology between family members raises strict requirement for selective analysis of miRNA. We have firstly prepared mismatched miRNAs with 100 folds concentration to that of target miR-21. Then, these miRNAs are detected by the proposed electrochemical method without and with the spiking of target miR-21. Electrochemical responses are measured. As shown in Fig. 3, in the absence of miR-21, these

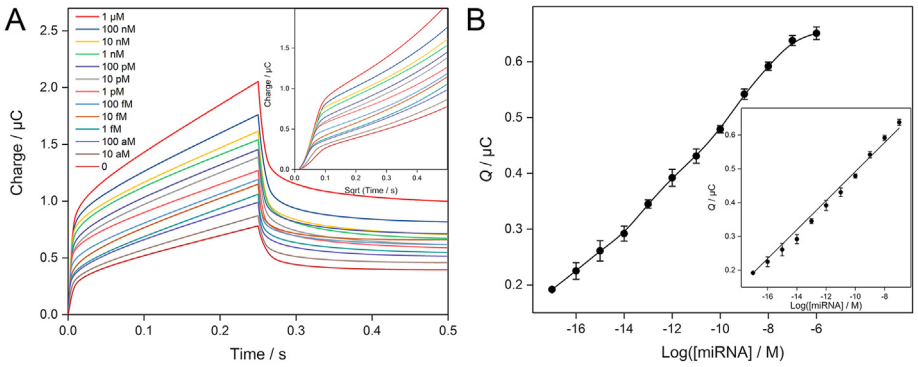

Fig. 2. (A) Chronocoulometry curves for the detection of miRNA with the concentrations of 0, 10^{-17}, 10^{-16}, 10^{-15}, 10^{-14}, 10^{-13}, 10^{-12}, 10^{-11}, 10^{-10}, 10^{-9}, 10^{-8}, 10^{-7}, 10^{-6} M. Inset is the chronocoulometry curves of charge versus time$^{1/2}$. (B) Calibration plot for miRNA concentration determinations. Inset shows the linear range.

Table 1
Comparison of the analytical performances of recent miRNA assays.

Technique	Strategy	Detection range (M)	LOD (M)	Ref
fluorescence	competitive hybridization resulted quenching	3.8×10^{-12} to 10^{-8}	3.8×10^{-12}	[30]
SWV	polydopamine-Au composite	10^{-12} to 10^{-8}	2.6×10^{-13}	[31]
CC	Au-loaded nanoporous superparamagnetic nanocubes	10^{-13} to 10^{-6}	10^{-13}	[32]
SWV	hairpin self-assembly recycling reaction	2×10^{-15} to 5×10^{-10}	1.6×10^{-15}	[33]
SPR	catalytic growth of AuNPs	8×10^{-16} to 2×10^{-12}	8×10^{-16}	[34]
DPV	Pd@UiO-66 and CHA	2×10^{-14} to 6×10^{-10}	7.13×10^{-16}	[35]
DLS	rolling circle amplification and AuNPs aggregation	10^{-15} to 10^{-8}	1.1×10^{-16}	[36]
EIS	polyoxometalate-derived MoS_2 nanosheets	10^{-15} to 5×10^{-9}	1.1×10^{-16}	[37]
ECL	multinary Zn–Ag–In–S/ZnS nanocrystals	10^{-16} to 2×10^{-11}	5×10^{-17}	[38]
ECL/SWV	DSN and CHA	10^{-16} to 10^{-10}	~3×10^{-17}	[39]
CC	TDNA-AuNPs tags and CHA	10^{-17} to 10^{-7}	10^{-17}	this work

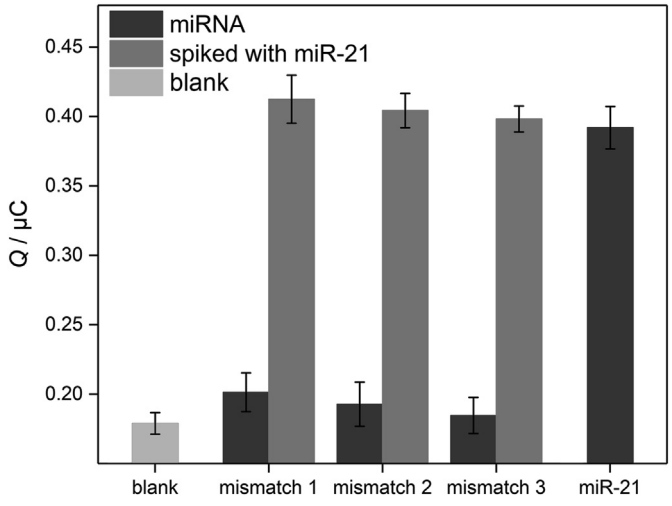

Fig. 3. Selectivity investigation for the analysis of different miRNA (miR-21: 1 pM, mismatched miRNAs: 100 pM).

mismatched miRNAs cannot effectively initiate SDA and subsequently CHA for the immobilization of tags. Therefore, the *Q* values are comparable with blank case. However, after adding target miR-21, although its concentration is only one percent of mismatched ones, remarkable *Q* values are obtained which are close to the corresponding value in the standard curve. These results demonstrate that mismatched miRNAs display negligible effects on the CC response towards target miRNA and high selectivity is promised. To validate the utility of this method for real sample analysis, standard addition method is applied using clinical human serum samples. 10, 100, and 1000 pM standard miR-21 are spiked in the samples before measurements. As shown in Table 2, the relative standard errors are below 6% and the recovery rate is from 99.7% to 114.0%. The satisfactory results suggest acceptable analysis capability of this method for biological samples. In addition, we have carried out standard qRT-PCR method to further check the accuracy of the electrochemical method. After comparison in Table 2, the results obtained by the two methods show excellent consistency. Therefore, the proposed work may have great practical utility for clinical analysis.

4. Conclusions

In summary, this work presents an electrochemical system for the detection of miRNA using TDNA modified AuNPs tags for the enhancement of electrochemical responses. SDA and CHA is smartly conjugated. The product of previous process is responsible for the recruitment of electrochemical tags on the surface of the electrode through recycled CHA. Compared with some previous strategies, this design not only integrates two recycling reactions without additional fuel strands, but also automatically locate multiple signal enhancers (tags) for output. Therefore, significantly improved analytical performances can be achieved. The recorded electrochemical signal is positively correlated with miRNA concentration. Due to the association of the signal amplification elements, the biosensor shows a low LOD of 10 aM. It also displays some apparent merits including high selectivity, good stability feasible operation and so on. The detection system eliminates the interference of complex components and performs satisfactorily in real samples. Therefore, it is anticipated that this method shows promising application prospects in biological researches and clinical diagnosis.

Table 2
Comparison of the detection results of human serum samples with the standard qRT-PCR measurements.

Sample	Spiked (pM)	Detected (pM)	qRT-PCR (pM)	Recovery (%)	Relative error (%)
1	1000	996.5	1003.8	99.7	4.5
	100	102.8	105.6	102.8	5.2
	10	11.4	12.5	114.0	3.7
2	1000	1005.7	1007.2	100.6	2.4
	100	103.8	97.3	103.8	5.6
	10	10.9	11.3	109.0	4.8

CRediT authorship contribution statement

Hua Chai: Investigation, Data curation, Writing – original draft. **Mingyuan Wang:** Data curation, Writing – original draft. **Longhai Tang:** Formal analysis, Data curation. **Peng Miao:** Conceptualization, Writing – review & editing, Project administration.

Declaration of competing interest

The authors declare that they have no known competing financial interests or personal relationships that could have appeared to influence the work reported in this paper.

Acknowledgments

This work was supported by the Science and Technology Cooperation Project between the Chinese and Australian Governments (2017YFE0132300), the Science and Technology Project of Ji Hua Laboratory (X190191TD190), the Training Program of Gusu Health Talents (GSWS2019023 and GSWS2019073), the Science and Technology Program of Suzhou (SS2019077) and the Health Science and Technology Program of Suzhou (GWZX202004).

Appendix A. Supplementary data

Supplementary data to this article can be found online at https://doi.org/10.1016/j.aca.2021.338543.

References

[1] L. He, G.J. Hannon, Micrornas: small RNAs with a big role in gene regulation, Nat. Rev. Genet. 5 (2004) 522–531.
[2] R.W. Carthew, E.J. Sontheimer, Origins and mechanisms of miRNAs and siRNAs, Cell 136 (2009) 642–655.
[3] W. Filipowicz, S.N. Bhattacharyya, N. Sonenberg, Mechanisms of post-transcriptional regulation by microRNAs: are the answers in sight? Nat. Rev. Genet. 9 (2008) 102–114.
[4] J. Lu, G. Getz, E.A. Miska, E. Alvarez-Saavedra, J. Lamb, D. Peck, A. Sweet-Cordero, B.L. Ebet, R.H. Mak, A.A. Ferrando, J.R. Downing, T. Jacks, H.R. Horvitz, T.R. Golub, MicroRNA expression profiles classify human cancers, Nature 435 (2005) 834–838.
[5] X. Chen, Y. Ba, L.J. Ma, X. Cai, Y. Yin, K.H. Wang, J.G. Guo, Y.J. Zhang, J.N. Chen, X. Guo, Q.B. Li, X.Y. Li, W.J. Wang, Y. Zhang, J. Wang, X.Y. Jiang, Y. Xiang, C. Xu, P.P. Zheng, J.B. Zhang, R.Q. Li, H.J. Zhang, X.B. Shang, T. Gong, G. Ning, J. Wang, K. Zen, J.F. Zhang, C.Y. Zhang, Characterization of microRNAs in serum: a novel class of biomarkers for diagnosis of cancer and other diseases, Cell Res. 18 (2008) 997–1006.
[6] A. Cimmino, G.A. Calin, M. Fabbri, M.V. Iorio, M. Ferracin, M. Shimizu, S.E. Wojcik, R.I. Aqeilan, S. Zupo, M. Dono, L. Rassenti, H. Alder, S. Volinia, C.G. Liu, T.J. Kipps, M. Negrini, C.M. Croce, miR-15 and miR-16 induce apoptosis by targeting BCL2, Proc. Natl. Acad. Sci. U.S.A. 102 (2005) 13944–13949.
[7] L.S. Yang, B. Wang, Q.Q. Zhou, Y.R. Wang, X.G. Liu, Z.M. Liu, Z.Z. Zhan, MicroRNA-21 prevents excessive inflammation and cardiac dysfunction after myocardial infarction through targeting KBTBD7, Cell Death Dis. 9 (2018) 769.
[8] S.K. Miroshnichenko, O.A. Patutina, E.A. Burakova, B.P. Chelobanov, A.A. Fokina, V.V. Vlassov, S. Altman, M.A. Zenkova, D.A. Stetsenko, Mesyl phosphoramidate antisense oligonucleotides as an alternative to phosphorothioates with improved biochemical and biological properties, Proc. Natl. Acad. Sci. U.S.A. 116 (2019) 1229–1234.
[9] S. Kanno, K. Nosho, K. Ishigami, I. Yamamoto, H. Koide, H. Kurihara, K. Mitsuhashi, M. Shitani, M. Motoya, S. Sasaki, T. Tanuma, H. Maguchi, T. Hasegawa, Y. Kimura, I. Takemasa, Y. Shinomura, H. Nakase, MicroRNA-196b is an independent prognostic biomarker in patients with pancreatic cancer, Carcinogenesis 38 (2017) 425–431.
[10] J. Li, J. Xue, M. Ling, J. Sun, T. Xiao, X. Dai, Q. Sun, C. Cheng, H. Xia, Y. Wei, F. Chen, Q. Liu, MicroRNA-15b in extracellular vesicles from arsenite-treated macrophages promotes the progression of hepatocellular carcinomas by blocking the LATS1-mediated Hippo pathway, Canc. Lett. 497 (2021) 137–153.
[11] P.S. Mitchell, R.K. Parkin, E.M. Kroh, B.R. Fritz, S.K. Wyman, E.L. Pogosova-Agadjanyan, A. Peterson, J. Noteboom, K.C. O'Briant, A. Allen, D.W. Lin, N. Urban, C.W. Drescher, B.S. Knudsen, D.L. Stirewalt, R. Gentleman, R.L. Vessella, P.S. Nelson, D.B. Martin, M. Tewari, Circulating microRNAs as stable blood-based markers for cancer detection, Proc. Natl. Acad. Sci. U.S.A. 105 (2008) 10513–10518.
[12] H.Y. Liu, L. Li, L.L. Duan, X. Wang, Y.X. Xie, L.L. Tong, Q. Wang, B. Tang, High specific and ultrasensitive isothermal detection of microRNA by padlock probe-based exponential rolling circle amplification, Anal. Chem. 85 (2013) 7941–7947.
[13] F. Chen, C.H. Fan, Y.X. Zhao, Inhibitory impact of 3 '-terminal 2 '-0-methylated small silencing RNA on target-primed polymerization and unbiased amplified quantification of the RNA in arabidopsis thaliana, Anal. Chem. 87 (2015) 8758–8764.
[14] Q. Zhang, F. Chen, F. Xu, Y.X. Zhao, C.H. Fan, Target-triggered three-way junction structure and polymerase/nicking enzyme synergetic isothermal quadratic DNA machine for highly specific, one-step, and rapid microRNA detection at attomolar level, Anal. Chem. 86 (2014) 8098–8105.
[15] X. Li, X. Zhuang, J. Lu, A label-free mass spectrometry detection of microRNA by signal switching from high-molecular-weight polynucleotides to highly sensitive small molecules, Talanta 224 (2021) 121899.
[16] D. Li, L. Xia, Q.J. Zhou, L. Wang, D.M. Chen, X. Gao, Y. Li, Label-free detection of miRNA using surface-enhanced Raman spectroscopy, Anal. Chem. 92 (2020) 12769–12773.
[17] T.Y. Xue, W.Y. Liang, Y.W. Li, Y.H. Sun, Y.J. Xiang, Y.P. Zhang, Z.G. Dai, Y.H. Duo, L.M. Wu, K. Qi, B.N. Shiyananju, L.J. Zhang, X.Q. Cui, H. Zhang, Q.L. Bao, Ultrasensitive detection of miRNA with an antimonene-based surface plasmon resonance sensor, Nat. Commun. 10 (2019) 28.
[18] X.M. Miao, Z.Y. Cheng, H.Y. Ma, Z.B. Li, N. Xue, P. Wang, Label-free platform for microRNA detection based on the fluorescence quenching of positively charged gold nanoparticles to silver nanoclusters, Anal. Chem. 90 (2018) 1098–1103.
[19] L. Tian, J.X. Qi, X.Y. Ma, X.J. Wang, C. Yao, W. Song, Y.H. Wang, A facile DNA strand displacement reaction sensing strategy of electrochemical biosensor based on N-carboxymethyl chitosan/molybdenum carbide nanocomposite for microRNA-21 detection, Biosens. Bioelectron. 122 (2018) 43–50.
[20] Y.X. Zhao, F. Chen, Q. Li, L.H. Wang, C.H. Fan, Isothermal amplification of nucleic acids, Chem. Rev. 115 (2015) 12491–12545.
[21] Y.T. Zhou, Q. Huang, J.M. Gao, J.X. Lu, X.Z. Shen, C.H. Fan, A dumbbell probe-mediated rolling circle amplification strategy for highly sensitive microRNA detection, Nucleic Acids Res. 38 (2010) e156.
[22] S. Bi, S.Z. Yue, S.S. Zhang, Hybridization chain reaction: a versatile molecular tool for biosensing, bioimaging, and biomedicine, Chem. Soc. Rev. 46 (2017) 4281–4298.
[23] X.F. Wang, X.L. Chen, C.X. Chu, Y.Y. Deng, M. Yang, Z. Ji, F.L. Xu, D.Q. Huo, Y. Luo, C.J. Hou, Four-stage signal amplification for trace ATP detection using allosteric probe-conjugated strand displacement and CRISPR/Cpf1 trans-cleavage (ASD-Cpf1), Sensor. Actuator. B Chem. 323 (2020) 128653.
[24] S.Z. Yue, T.T. Zhao, H.J. Qi, Y.C. Yan, S. Bi, Cross-catalytic hairpin assembly-based exponential signal amplification for CRET assay with low background noise, Biosens. Bioelectron. 94 (2017) 671–676.
[25] C. Avendano, M.A. Patarroyo, Loop-mediated isothermal amplification as point-of-care diagnosis for neglected parasitic infections, Int. J. Mol. Sci. 21 (2020) 7981.
[26] P. Miao, Y.G. Tang, Z.Q. Mao, Y.Z. Liu, Adamantane derivatives functionalized gold nanoparticles for colorimetric detection of MiRNA, Part. Part. Syst. Char. 34 (2017) 1600405.
[27] T. Tian, J. Li, C. Xie, Y.H. Sun, H.Z. Lei, X.Y. Liu, J.Y. Xia, J.Y. Shi, L.H. Wang, W.Y. Lu, C.H. Fan, Targeted imaging of brain tumors with a framework nucleic acid probe, ACS Appl. Mater. Interfaces 10 (2018) 3414–3420.
[28] D.W. Yang, L.M. Ning, T. Gao, Z.H. Ye, G.X. Li, Enzyme-free dual amplification strategy for protein assay by coupling toehold-mediated DNA strand displacement reaction with hybridization chain reaction, Electrochem.

Commun. 58 (2015) 33–36.
[29] Z.H. Ye, B. Zhang, Y.C. Yang, Z.X. Wang, X.L. Zhu, G.X. Li, Electrochemical biosensor for the nuclear factor kappa B using a gold nanoparticle-assisted dual signal amplification method, Microchim. Acta 181 (2014) 139–145.
[30] W. Wang, T. Kong, D. Zhang, J. Zhang, G.S. Cheng, Label-free microRNA detection based on fluorescence quenching of gold nanoparticles with a competitive hybridization, Anal. Chem. 87 (2015) 10822–10829.
[31] S.-C. Chen, K.-T. Chen, A.F.-J. Jou, Polydopamine-gold composite-based electrochemical biosensor using dual-amplification strategy for detecting pancreatic cancer-associated microRNA, Biosens. Bioelectron. 173 (2021) 112815.
[32] M.K. Masud, M.N. Islam, M.H. Haque, S. Tanaka, V. Gopalan, G. Alici, N.T. Nguyen, A.K. Lam, M.S.A. Hossain, Y. Yamauchi, M.J.A. Shiddiky, Gold-loaded nanoporous superparamagnetic nanocubes for catalytic signal amplification in detecting miRNA, Chem. Commun. 53 (2017) 8231–8234.
[33] J.L. Li, Z.P. Chen, Y. Xiang, L.L. Zhou, T. Wang, Z. Zhang, K.X. Sun, D. Yin, Y. Li, G.M. Xie, An electrochemical biosensor for double-stranded Wnt7B gene detection based on enzymatic isothermal amplification, Biosens. Bioelectron. 86 (2016) 75–82.
[34] W.Y. Nie, Q. Wang, L.Y. Zou, Y. Zheng, X.F. Liu, X.H. Yang, K.M. Wang, Low-fouling surface plasmon resonance sensor for highly sensitive detection of microRNA in a complex matrix based on the DNA tetrahedron, Anal. Chem. 90 (2018) 12584–12591.
[35] T.J. Meng, N.Z. Shang, A. Nsabimana, H.M. Ye, H. Wang, C. Wang, Y.F. Zhang, An enzyme-free electrochemical biosensor based on target-catalytic hairpin assembly and Pd@UiO-66 for the ultrasensitive detection of microRNA-21, Anal. Chim. Acta 1138 (2020) 59–68.
[36] Y. Gao, S.Y. Xu, T. He, J.W. Li, L.S. Liu, Y.Y. Zhang, S.G. Ge, M. Yan, H.Y. Liu, J.H. Yu, Ultrasensitive and specific microRNA detection via dynamic light scattering of DNA network based on rolling circle amplification, Sensor. Actuator. B Chem. 324 (2020) 128693.
[37] Q.J. Jia, S.J. Huang, M.Y. Hu, Y.P. Song, M.H. Wang, Z.H. Zhang, L.H. He, Polyoxometalate-derived MoS2 nanosheets embedded around iron-hydroxide nanorods as the platform for sensitively determining miRNA-21, Sensor. Actuator. B Chem. 323 (2020) 128647.
[38] B. Zhang, F. Zhang, P. Zhang, D.Z. Shen, X.W. Gao, G.Z. Zou, Ultrasensitive electrochemiluminescent sensor for microRNA with multinary Zn-Ag-In-S/ZnS nanocrystals as tags, Anal. Chem. 91 (2019) 3754–3758.
[39] L.P. Zhu, M.Q. Zhang, J. Ye, M.X. Yan, Q.J. Zhu, J.S. Huang, X.R. Yang, Ratiometric electrochemiluminescent/electrochemical strategy for sensitive detection of microRNA based on duplex-specific nuclease and multilayer circuit of catalytic hairpin assembly, Anal. Chem. 92 (2020) 8614–8622.